

Smart Manufacturing and Material Processing (SMMP)

DOI: http://doi.org/10.26480/smmp.01.2023.06.10





RESEARCH ARTICLE

MICROSTRUCTURE EVOLUTION OF TIN COATINGS PREPARED BY DUAL-PULSE POWER MAGNETRON SPUTTERING

Chao Yang^a, Juan Hao^{a*}, Baichuan Wang^a, Yuhang Ding^a, Jing Zhang^a, Dan Dong^a, O.O. Oluwoleb^b

- ^a Xi'an University of Technology, School of Materials Science and Engineering, Xi'an 710048, China
- ^b Department of Mechanical Engineering, University of Ibadan, Nigeria
- *Corresponding Author Email: haojuan19901207@163.com

This is an open access article distributed under the Creative Commons Attribution License CC BY 4.0, which permits unrestricted use, distribution, and reproduction in any medium, provided the original work is properly cited.

ARTICLE DETAILS

Article History:

Received 20 January 2024 Revised 18 February 2024 Accepted 11 March 2024 Available online 13 March 2024

ABSTRACT

The type of power source and the deposition parameters directly determine the growth structure of the coating during the magnetron sputtering, resulting in the difference of the mechanical properties of the coating. High power impulse magnetron sputtering (HIPIMS) generates high-density plasma by high power pulsed power source, which leads to the coating with dense structure and excellent mechanical properties. However, the low deposition rate of HIPIMS reduces the coating preparation efficiency and affects its industrial application. Therefore, dual-pulse power magnetron sputtering technology has been developed to improve the deposition rate and quality of coatings. In this study, TiN coatings were prepared using DPPMS at different deposition times. The microstructure, deposition rate, residual stress and adhesion of TiN coatings were analyzed. The results showed that when only one target was used for deposition, the deposition rate of TiN coatings increased first and then decreased during the coating growth. When the deposition time was 80 min, the deposition rate reached the maximum value of 52 nm/min. After the deposition time of 80 min, the residual stress in the TiN coatings changed from compressive stress to tensile stress, resulting in a significant decrease in the deposition rate of TiN coatings. The microstructure of TiN coatings gradually changed from fibrous structure to dense columnar structure with the prolongation of deposition time. In addition, when the deposition time was 80 min, the TiN coating had low residual compressive stress (-0.2 GPa), high hardness (27.5 GPa) and elastic modulus (340 GPa), and excellent adhesion between the coating and the substrate.

KEYWORDS

HIPIMS; DPPMS, TiN coating, microstructure, deposition rate

1. Introduction

In recent years, high power impulse magnetron sputtering (HIPIMS), as an alternative to di-rect current magnetron sputtering (DCMS), has attracted extensive attention from many re-searchers and the industry (Purandare et al., 2020; Chen et al., 2019). It utilizes high peak target power and extremely low duty cycle to generate high-density plasma and highly ionized sputtered particles to improve the microstructure and mechanical properties of coatings (Badini et al., 2019; Wu et al., 2019). However, the deposition rate of transition metal nitride coatings deposited by HIPIMS is only 15%-50% compared with that of DCMS at the same average target power because the sputtered ions can be attracted back toward the cathodic target, low duty cycle and target poisoning (Lin et al., 2017; Bleykher et al., 2018). In addi-tion, the residual stress generated during the coating deposition process also reduces the dep-osition rate and weakens the adhesion between the substrate and the coating (Guimaraces et al., 2018; Xi et al., 2017). These defects seriously affect the industrialization of

In order to overcome the deposition rate loss problem of HIPIMS, dualpulse power magne-tron sputtering (DPPMS) has been developed, and the schematic of electric field is shown in Figure 1. The different between the HIPIMS and DPPMS technique is that one overall pulse period in DPPMS has two independent pulse stages, and the parameters of the two pulse stages (such as power, voltage, current, duty cycle, etc.) can be adjusted arbitrarily to obtain stable plasma discharge process and different plasma characteristics. To increase plasma den-sity and deposition rate, the first pulse stage applies low power and long duty cycle to the target to ignite the plasma and perform pre-deposition. Then the second pulse stage produces a high-density plasma and sputtered particles with high target power and appropriate duty cycle. The plasma generated in the first pulse stage can increase the impact ionization rate of working gas atoms in the second pulse stage, resulting in a higher target current density or plasma density under the same target power condition. Furthermore, prolonging the low-intensity sputtering process in the first pulse stage can reduce target poisoning during the deposition of nitride coatings and increase the deposition rate in the second pulse stage (Hao et al., 2020).

In this study, TiN coatings were deposited using DPPMS at different deposition times. The effect of deposition time on the microstructure, deposition rate, residual stress and adhesion of TiN coatings was investigated. In addition, the growth process and structural evolution of TiN coatings deposited using DPPMS were discussed in detail. The research results provide theoretical and experimental support for the development of electric field of magnetron sput-tering technology.

Quick Response Code Access this article online



Website:

Website: www.topicsonchemeng.org.my

DOI:

10.26480/smmp.01.2023.06.10

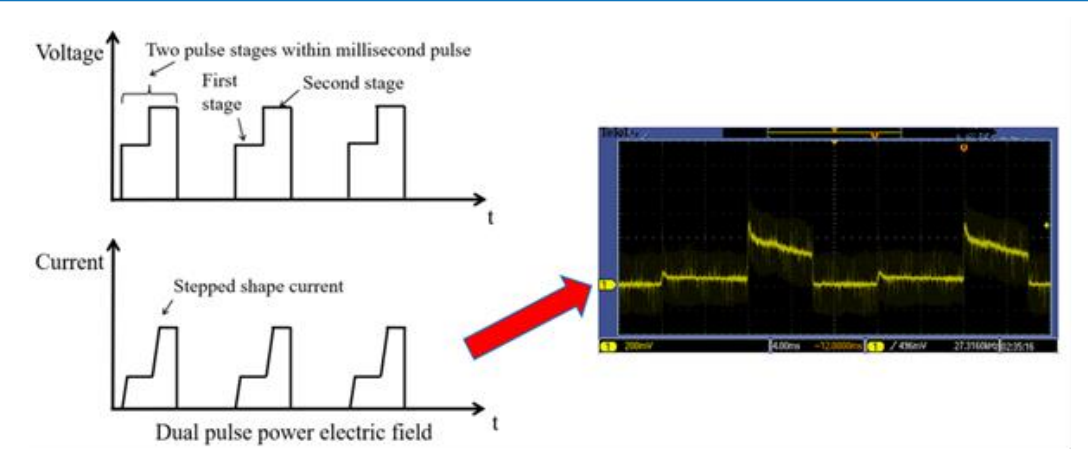


Figure 1: The schematic diagram of the voltage and current waveforms of DPPMS and the current measurement diagram

2. EXPERIMENT

TiN coatings were deposited from a metal Ti target (2170 mm2H7 mm, purity 99.9%) using dual pulsed power (DPP) source in an unbalanced closed field magnetron sputtering system. The maximum target power of the DPP was 12 kW, and the duty cycle could be set from 5% to 100%. 304 stainless steel and (100) Si wafer were installed 140 mm away from the Ti tar-get. Prior to deposition, substrates were sputtered by Ar+ plasma bombardment at -400 V bias. A 200 nm Ti adhesion layer and the following TiN coatings were deposited in an Ar (85 sccm) and Ar/N2 mixture (65 and 20 sccm), respectively. The working pressure was set to be 0.6 Pa. A -60 V dc substrate bias was used for all depositions. During the formal sedimentation pro-cess, dual-pulse stages were used. The average target power and pulse width of the first pulse stage and the second pulse stage were 0.2 kW and 6 ms, 3.0 kW and 6 ms, respectively. The average target current and voltage during the second pulse stage were 6 A and 500 V. The pulse frequency was fixed at 50 Hz. The deposition time was selected as 20, 40, 60, 80 and 100 minutes. The temperatures in the vacuum chamber after deposition at different times were 56, 60, 68, 73 and 80 °C, respectively. Only one Ti Target was used during the deposition process.

The microstructure morphology of TiN coatings was investigated by scanning electron micro-scope (JSM-6700F). The phase composition was characterized by X-ray diffraction (XRD-7000S). The grain size was calculated by Scherrer formula. The residual stress of TiN coatings was calculated by X-ray diffractometer $\sin 2\psi$ method. The hardness and elastic modulus of coatings were measured by nanoindenter device (G200). The adhesion was eval-uated by surface indentation experiment.

3. RESULTS AND DISCUSSION

3.1 Microstructure

Figure 2 showed the surface and cross-sectional SEM images of TiN coatings deposited for different times. The coating exhibited cauliflower-like clusters and fibrous structure at the ini-tial deposition stage. A large number of micro-gaps between clusters were observed. As depo-sition continued, the fibrous structure transformed into columnar structure (Figure 2a to 2e). The size of clusters increased slightly, and the clusters were more compact, thus proving the gradual increase in the compactness of TiN coatings. The reason for this phenomenon was the gradual increase of the deposition temperature and the increased activity of the sputtered par-ticles.

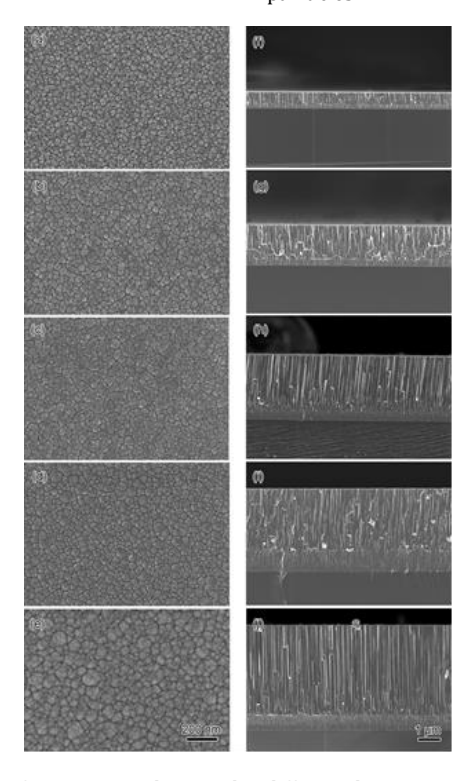


Figure 2: Surface and cross-sectional SEM images of TiN coatings deposited at different deposition time (a) (f) 20 min, (b) (g) 40 min, (c)(h) 60 min, (d) (i) 80 min, (e) (j) 100 min

The XRD pattern of TiN coatings was shown in Figure 3. The diffraction peaks appeared at 36.7°, 42.6°, and 61.8°, which corresponded to (111), (200), and (220) crystal planes of TiN with face centered cubic (fcc) structure. No diffraction peaks of Ti and Ti2N were detected. The intensity of diffraction peaks gradually increased with the extension of deposition

time, indicating that the degree of crystallization and grain size of the coating gradually increased. The average grain sizes of TiN coatings calculated from (111) and (220) crystal planes were 10, 12, 13, 15, 18 nm, respectively.

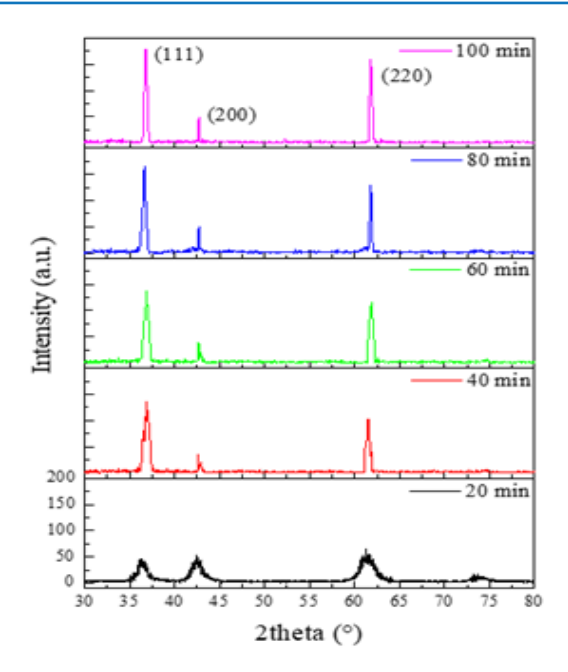


Figure 3: XRD pattern of TiN coatings deposited at different deposition time

The characteristics of the dual pulse power (DPP) and deposition time were the main factors affecting the crystal structure and microstructure of TiN coatings. In this study, a low target power of 0.2~kW and a long duty cycle of 30% were set in the first pulse stage of the DPP, which could not

only achieve the pre-deposition of TiN coatings, but also increase the substrate temperature. This process could enhance adsorption of sputtered particles on the sub-strate surface and improve its mobility. The second pulse stage with a high target power of 3 kW could generate a large amount of high energy plasma, and plasma transferred high energy to the adatoms on the substrate surface, which could increase the number of nucleation and promote polycrystalline growth of TiN coatings. On the other hand, according to the classical structure theory of coatings, at the initial deposition, lower deposition temperature and lower bulk diffusion energy of adatoms led to the growth of the TiN coating with fibrous structure and micro-gaps (Zhang et al., 2014). As sedimentation time increases, the effect of plasma bombardment on the substrate surface was gradually enhanced, thereby improving the bulk diffusion energy and mobility of adatoms, and the dense columnar structure could be depos-ited. Enhancing the mobility of adatoms could also increase the driving force for grain growth and the preferential growth of TiN coatings on the (111) plane, which had the lowest strain energy (Liang et al., 2016). At the same time, due to the high deposition rate and enhanced plasma bombardment, the growth of the TiN coating took the (220) plane with the lowest stopping energy as the preferred orientation. In other words, due to lower sputtering yield, the (220) plane could survive under the ion bombardment, while other planes were preferen-tially sputtered away (Zhao et al., 2015). Therefore, both (111) and (220) planes were the pre-ferred orientations of TiN coatings.

3.2 Deposition Rates and Residual Stress

The thicknesses of TiN coatings were 892, 1855, 2916, 4140 and 4733 nm at different depo-sition times. Figure 4 showed the residual stress and deposition rate of TiN coatings. The deposition rate first increased and then decreased. The deposition rate reached a maximum value of 52 nm/min when the deposition time was 80 min. In addition, the residual stress in-side the coating changed from compressive stress (-1.3 GPa) to tensile stress (0.4 GPa) with increasing deposition time.

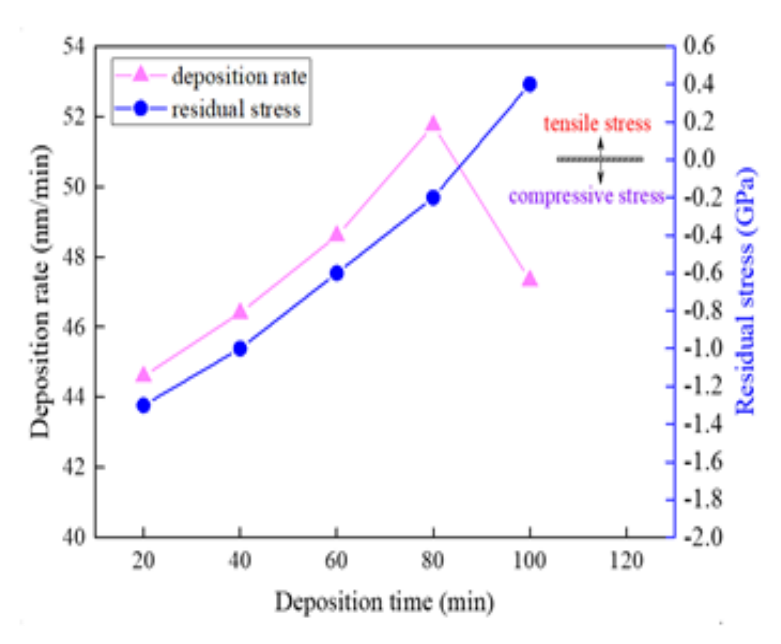


Figure 4: Deposition rate and residual stress of TiN coatings

Plasma bombardment and structural changes during coating growth were the main reasons for the induced residual stress (Tillman et al., 2021). In the DPPMS deposition, since the low-density plasma generated by applying low power and long duty cycle to the target during the first pulse stage was favorable for further ionization of the plasma, the high-density plas-ma was obtained when high power was applied to the target in the second pulse stage. High-density plasma composed of working gas ions (Ar+) and sputtered ions (Ti+) continu-ously bombarded the growth interface of the coating, resulting in a large compressive stress. Therefore, TiN coatings with deposition times less than 80 min exhibited compressive stress. In addition, the TiN coating exhibited an increasing tensile stress with the increase of coating thickness due to the existence of a large number of lattice mismatched grain boundaries or defects in the TiN coating with polycrystalline structure. When the deposition time was 100 min, the residual tensile stress of the TiN coating was 0.4 GPa. On the other hand, in the magnetron sputtering process, the deposition rate of the coating was mainly affected by the sputtering yield, target power and deposition parameters. In this study, the sputtering yield and target power were kept constant. The deposition temperature increased slightly as the deposition

time increased, which improved the adsorption of sputtered particles on the sub-strate surface, resulting in a slight increase in the deposition rate. However, when the deposition time increased from 80 to 100 min, the coating peeled off during the coating growth due to residual tensile stress, resulting in a decrease in the deposition rate from 52 to 47 nm/min.

3.3 Hardness and Adhesion

Hardness and elastic modulus were important and valuable parameters used to evaluate the mechanical property of TiN coatings, as shown in Table 1. When the deposition time was changed from 20 to 80 min, the hardness and elastic modulus increased from 22.8 and 292 GPa to 27.5 and 340 GPa. When the deposition time was 100 min, the hardness and elastic modulus decreased slightly. Hardness was affected by factors such as chemical composition, microstructure, residual stress and so on . Due to the approximate deposition parameters, the main factors affecting hardness in this study were microstructure and residual stress. When the deposition time was 80 min, the TiN coating had a dense microstructure and small residual compressive stress, which was beneficial to the improvement of hardness and elastic modulus.

Table 1: The performance parameters of TiN coatings						
Sample ID	Deposition Time (min)	Grain Size (nm)	Residual Stress (GPa)	Hardness (GPa)	Elastic Modulus (GPa)	Deposition Rate (nm/min)
TiN-1	20	10	-1.3	22.8	292	44.6
TiN-2	40	12	-1.0	25.2	323	46.4
TiN-3	60	13	-0.6	25.8	331	48.6
TiN-4	80	15	-0.2	27.5	340	52.0
TiN-5	100	18	0.4	26.2	333	47.3

The adhesion between the coating and substrate is an important factor determining the per-formance, durability, and reliability of coated engineering parts. The Rockwell hardness in-dentation test was used to evaluate adhesion, and the optical micrographs of the indentation was shown in Figure 5. Coating chipping and cracking were observed at the indentation edge of the TiN coating deposited for 20 min. With the prolongation of deposition time, the inden-tation edge was relatively smooth and flat, and there were no obvious chips or cracks. When the deposition time was 100 min, small areas of coating chipping were observed. Combined with the evaluation criteria of indentation morphology, when the deposition time increased from 20 to 100 min, the corresponding adhesion grades were HF5, HF0, HF0, HF0, HF2, respectively.

For soft substrate (304 stainless steel) and hard coating (TiN coating), the different plastic deformations of the substrate and coating make the

indentation behavior more complex. Sub-strate and coating usually used plastic deformation to release strain energy concentration gen-erated during indentation (Meng et al., 2019). However, due to limited deformability, hard coating might form cracks or chips in the indentation area. Therefore, it was necessary to pre-pare a transition coating (Ti coating) between the soft substrate and hard coating to improve the adhesion (Xie et al., 2019). In this study, the TiN coating deposited for 20 min exhibited higher residual stress, which caused the coating to be more prone to cracks and chips during plastic deformation at the indentation edge, resulting in poor adhesion. With the increase of deposition time, the thickness of the coating gradually increased and the residual stress decreased, which effectively enhanced the adhesion. However, As the deposition time increased to 100 min, residual tensile stress was formed in the coating due to lattice mismatch or struc-tural defects, which weakened the adhesion.

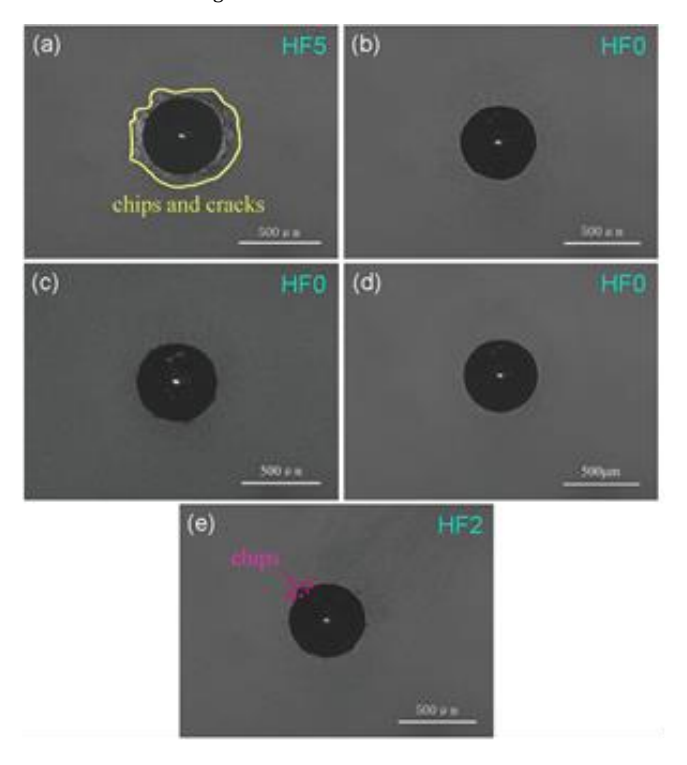


Figure 5: The optical micrographs of indentation of TiN coatings at different deposition time (a) 20 min; (b) 40 min; (c) 60 min; (d) 80 min; (e) 100 min

4. CONCLUSION

As the deposition time increases, the microstructure of TiN coating gradually changed from fibrous structure to dense columnar structure. All TiN coatings exhibited polycrystalline structure with preferred orientation of (111) and (220) planes.

When the deposition time was $80 \, \text{min}$, the maximum deposition rate of the TiN coating was $52 \, \text{nm/min}$. The TiN coating had low residual compressive stress (-0.2 GPa), high hardness (27.5 GPa) and elastic modulus (340 GPa), and excellent adhesion between the coating and the substrate.

ACKNOWLEDGEMENTS

This research work is financially supported by Xi'an Science and Technology Plan Project (No. 23GXFW0055), National Natural Science Foundation of China (No. 52001251), Shaanxi Provincial Natural Science Basic Research Program Project (No. 2024JC-YBQN-0525), Chi-na Postdoctoral Science Foundation (No. 2021M692597) and Natural Science Foundation of the Education Department (No. 21JK0799). We thank the

reviewers for their informative and insightful suggestions regarding our work.

REFERENCES

Badini, C., Deambrosis, S.M., Padovano, E., 2019. Thermal shock and oxidation behavior of HiPIMS TiAlN coatings grown on Ti-48Al-2Cr-2Nb intermetallic alloy. Materials, 9, Pp. 961

Bleykher, G.A., Sidelev, D.V., Grudinin, V.A., 2018. Surface erosion of hot Cr target and deposition rates of Cr coatings in high power pulsed magnetron sputtering. Surface and Coatings Technology, 354, Pp. 161.

Chen, Y.I., Zheng, Y.Z., Chang, L.C., 2019. Effect of bias voltage on mechanical properties of HiPIMS/RFMS cosputtered Zr-Si-N films. Materials, 12, Pp. 2658.

Guimaraes, M.C., Castilho, B.C., Nossa, T.S., 2018. On the effect of substrate oscillation on CrN coatings deposited by HiPIMS and dcMS. Surface and Coatings Technology, 340, Pp. 112.

- Hao, J., Jiang, B.L., Yang, C., 2020. Effect of target current of dual-stage HPPMS on the mi-crostructure and corrosion resistance of TiN coatings. Rare Metal Materials and Engineer-ing, 49, Pp. 2991.
- Liang, H.L., Xu, J., Zhou, D.Y., 2016. Thickness dependent microstructural and electrical properties of TiN thin films prepared by DC reactive magnetron sputtering. Ceramics In-ternational, 42, Pp. 2642.
- Lin, T.G., Wang, J., Liu, G., 2017. Influence of discharge current on phase transition proper-ties of high quality polycrystalline VO2 thin film fabricated by HiPIMS. Materials, 10, Pp. 633.
- Meng, D., Li, Y.G., Jiang, Z.T., 2019. Scratch behavior and FEM modelling of Cu/Si(100) thin films deposited by modulated pulsed power magnetron sputtering. Surface and Coat-ings Technology, 363, Pp. 25.
- Purandare, Y.P., Ehiasarian, A.P., Stack, M.M., 2020. CrN/NbN coatings deposited by HIPIMS: A preliminary study of erosion-corrosion performance. Surface and Coatings Technology, 204, Pp. 1158
- Tillmann, W., Grisales, D., Stangier, D., 2021. Residual stresses and tribomechanical behav-iour of TiAlN and TiAlCN monolayer and

- multilayer coatings by DCMS and HiPIMS. Surface and Coatings Technology, 406, Pp. 126664.
- Wu, W.Y., Chan, M.Y., Hsu, Y.H., 2019. Bioapplication of TiN thin films deposited using high power impulse magnetron sputtering. Surface and Coatings Technology, 362, Pp. 167.
- Xi, Y.T., Gao, K.W., Pang, X.L., 2017. Film thickness effect on texture and residual stress sign transition in sputtered TiN thin films. Ceramics International, 43, Pp. 11992.
- Xie, Q., Fu, Z.Q., Wei, X., 2019. Effect of substrate bias current on structure and properties of CrNx films deposited by plasma enhanced magnetron sputtering. Surface and Coatings Technology, 365, Pp. 134.
- Zhang, P., Zhang, J.Y., Li, J., 2014. Microstructural evolution, mechanical properties and de-formation mechanisms of nanocrystalline Cu thin films alloyed with Zr. Acta Materialia, 76, Pp. 221.
- Zhao, Y.H., Guo, C.Q., Yang, W.J., 2015. TiN films deposition inside stainlesssteel tubes us-ing magnetic field-enhanced arc ion plating. Vacuum, 112, Pp. 46.

